HARDNESS AND FRATURE TOUGHNE OF PLASMA SPRAYED ZIRCONIA-CERIA-YTTRIA THERMAL BARRIER COATINGS

Mohammed Jasim Kadhim Mohammed Hliyil Hafiz Maryam Abduladeem Ali Bash
Department of Production Engineering and Metallurgy
University of Technology, Baghdad, Iraq
+ College of Engineering, Al-Iraqi University
maryam_uot@yahoo.com

ABSTRACT

Several studies have been made during the recent years to evaluate the plasma sprayed yttria partially stabilized zirconia thermal barrier coatings but less attention were undertaken on ceria-yttria stabilized zirconia. In this study, zirconia- 20 wt% ceria-3.6 wt% yttria thermal barrier coatings were produced by air plasma spraying deposited on IN 738 LC superalloy substrate. The objective of this study is to analysis the distribution of porosity, hardness and fracture toughness on the deposited coatings. Under optimum plasma spraying conditions, it is dangerous to consider the mean values of hardness and fracture toughness. The distributions of hardness and fracture toughness are highly scattered. The Weibull distribution is the main parameter to describe the plasma sprayed coatings hardness and fracture toughness.

KEYWORDS : ceria-yttria stabilized zirconia; plasma sprayed coating; hardness; Fracture toughness; Weibull's modulus

الصلادة وعساوة الكسر لطبقات الرش بالبلازما للحواجز الحرارية للزركونيا-سيريا-ياتريا

محمد جاسم كاظم محمد هليل حافظ مريم عبد العظيم باقر علي باش
الجامعة التكنولوجية/ قسم الانتاج والمعادن

الخلاصة

اجريت خلال السنوات الاخيرة العديد الدراسات لتقييم طبقات الرش بالبلازما للحواجز الحرارية للياتريا المثبتة جزئيا للزركونيا لكن اهتمام اقل تم ايلائه للسيريا المثبتة للزركونيا. في هذه الدراسة تم انتاج طلاءات من الحواجز الحرارية للزركونيا- 20 wt% سيريا- 3.6 wt% ياتريا على ارضية من السبيكة الفائقة نوع IN 738 LC. ان الهدف لهذه الدراسة هو تحليل توزيع المسامية والصلادة وعساوة الكسر في الطلاءات الناتجة. تحت ظروف الطلاء المثلى فانه من الخطورة اعتماد القيم الوسطى للصلادة وعساوة الكسر. ان قيم الصلادة وعساوة الكسر تتستت بصورة كبيرة. ان توزيع ويبل هو المعامل الاساسي لوصف صلادة وعساوة الكسر لطبقات الرش بالبلازما .

Received: 2017 - 5 - 31
Accepted: 2017 - 9 - 26

INTRODUCTION

For the last at least 80 years, the field of stability of zirconia ceramics with different oxides was progressed considerably Blairbarlett and Thomas Jr (1934), Miller (1997). These days, stabilizing of zirconia mainly with specific amounts of yttria are highly advanced and acknowledged by many academics and industrials personals as promising candidates for many mechanical, electrical, corrosion, oxidation, high temperature corrosion and thermal applications Saremi et al. (2008), Bai et al. (2011), Ramachandran et al. (2012), The most widely used products in high temperature advanced applications are plasma spray thermal barrier coatings for utility, diesel and gas turbine engines Strangman and Schienle (1990), Wang and Sayre (2009), Wang et al. (2011),. In spite of zirconia stabilized with magnesia (MgO) and calcia (CaO) were well known and investigated thoroughly the relatively recent stabilizing with yttria (Y_2O_3) and ceria (CeO_2) are advanced well Duwez and Brownn (1952), Hajizadeh (2016). It was established that high cooling rate processes of yttria partially stabilized zircon with 7-8.5 wt% yttria (such as plasma spray) have three interesting characteristics for thermal barrier coatings Bratton and Lau (1981), Tsipas (2010), Wang et al. (2012). These are nearly invariant high thermal expansion, phase stability (dependent on time and temperature of exposure) and low thermal diffusivity. Therefore, many scientific and industrial works had been carried out to enhance the performance of plasma sprayed thermal barrier coatings of yttria partially stabilized zirconia using many secondary techniques Wilden et al. (1998), Girolamo et al. (2010) . Many scientific efforts in the field of thermal barrier coatings are mainly concentrated on increasing the thrust gas turbine engine and increasing the lifetime of coatings Chang et al. (1987), Golosnoy et al. (2009), Chang et al. (1987). This may be achieved via developing successful cooling systems to substrate, enhancement of thermal shock resistance, increasing the resistance of hot corrosion at high temperature, and developing new systems based on ceria-yttria stabilized zirconia. The efficiency of advanced critically gas turbine engines based mostly on the maximum temperature that can be introduced as possible. These high temperatures would not only control by the ceramic coatings but also highly affected by the other coatings of the thermal barrier coatings systems Lee et al. (2000). It was well established that different thermal plasma spraying techniques are used effectively to obtain the necessary morphology and stable nonotransformable tetragonal (t') phase resisting the severe heating and cooling cycles Zhou et al. (2017). Unfortunately, the presence of porosity associated with the plasma technique has a drawback on high temperature corrosion resistance . From the above description appears that any secondary technique following plasma sprayed coating which eliminating the porosity and cracking may enhance the performance of the TBCs. This will be only successful if the other requirements of the system will not be altered; it means thermal, mechanical and chemical properties. The reproducibility is the most parameter should be determined for thermal barrier coatings since it describes the variation of the properties within the engine as well as within the different engines. Determine the values of properties scatter of plasma sprayed thermal barrier coatings are very important in order to describe and understand the reliability .

This paper is deigned to report the implement of Weibull's distribution as an essential data representation to describe the performance of plasma sprayed coating during manufacturing and application. It gives many features for designer to take vital decisions on the quality of the sprayed coating and finally selection the operating conditions to prevent catastrophic failure.

EXPERIMENTAL PROCEDURES

The thermal barrier coating system investigated in this study is based on superalloy substrate, standard plasma spray bond coat and plasma sprayed ceramic coat. The substrate is standard reliable superalloy TM IN-738 LC. The inner coat is the bond coat based on Amdry

963 powder (Ni-24.5 wt% Cr-6 wt% Al-0.4 wt% Y). The upper plasma sprayed ceramic coat is based on a premixed powder of Sulzer Metco 205NS (ZrO_2-25 wt% CeO_2-2.5 wt% Y_2O_3) and Sulzer Metco 204NS-G (ZrO_2-8 wt% Y_2O_3) powder. The final composition of the premixed powder is ZrO_2-20 wt% CeO_2-3.6 wt% Y_2O_3. The nominal ranges of bond coat (Amdry 963) and mixed powder (Sulzer Metco 205NS and Sulzer Metco 204NS-G) are -90 +45 µm and -125 +11 µm respectively. The thicknesses of the thermal barrier coating component are 3 mm substrate, 90 ± 15 µm bond coat and 400 ± 25 µm ceramic top coat; the diameter of the samples is 25 mm. Standard procedures of substrate preparation prior to plasma spraying are listed in Table(1). Atmospheric 3MB plasma spraying coating unit manufactured by Metco INC, Westury, L.I.N.Y company was used to plasma spray both the bond coat of Amdray 963 and the premixed Sulzer Metco 205NS and Sulzer Metco 204NS-G (80 wt% and 20 wt%) coat respectively onto the IN-378 LC superalloy. In order to design the experiments carefully to evaluate the reliability of the thermal barrier coatings, scientific selection of the most important dependent parameters were considered (Table 1). Many processing conditions were selected and many samples were manufactured and analyzed. The best processing plasma spraying sheet was used to investigate the samples to determine the scattering of the properties. The plasma arc generates between the anode and cathode due to ionization of primary gas (argon) and secondary gas (hydrogen). Different proportion rates of secondary gas were used for spraying the bond coat (15.25%) and ceramic layer (12.37%) respectively. The pressure of gases for both bond coat and ceramic coat were kept constant at 3.44 bars. All the processing parameters of plasma spraying are listed in Table 1. During plasma spraying argon inert gas was applied to the substrate to prevent unwanted reactions between the spraying powder particles and air and also to serve as cooling for substrate.

Single metering feeder system was used for the bond coat powder and then for the premixed ceramic powder. The feeder devise was adjusted carefully by means of argon gas carrier to deliver the given powder continuously through the feeding nozzle. The selected powder flow rate for bond coat and ceramic coat were 45 and 35 g/min respectively. The position of the given injected powder was perpendicular to the inner higher temperature plasma jet. This position of plasma jet interaction with the given powder will lead to melting of particles and accelerated them toward the substrate as well as to the jig to produce the coating.

The roughness of the upper surface plan view of the as-sprayed was measured. The values reported for roughness are the central line average (CLA). The test was performed using roughness tester type TR200. The average of at least five reading was taken. The cut-off lengths employed are 2 to 4 mm. Microhardness of as-sprayed coatings was measured from the polished upper surfaces using digital Vickers hardness tester TH714. The applied load was 500 g. The average hardness was made from Weibull's distribution at 37% survival. The fracture toughness was determined from the indentation method based of indenter diagonal and the average crack length initiated from the diagonal corners. It should be reported that the size of samples are relevant to evaluate the fracture toughness of the plasma sprayed and as-sealed coatings. The type of cracks produced is Palmqvist. The suitable reliable equation to calculate the fracture toughness from indentation test is the equation reported by Ponton and Rawlings (1989):

$$K_{Ic} = 0.0101\ P/a\ c^{0.5} \qquad (1)$$

where P is the applied load (4.9 N), a is the half length of the average indent (mm) and c is the length from the center of the indent to the end of the crack flow (mm).

RESULTS AND DISCUSSION

In order to describe the reliability of the plasma sprayed coating even under similar identical processing conditions, detail analysis of topography of upper surface plan view to determine the roughness was made. Fig. 1 shows the typical SEM micrographs of the upper surface plan views of plasma sprayed coating without any metallographic preparations. The thoroughly microstructure investigated at different regions on the samples and also from different samples have been demonstrated the complex nature of the CYSZ ceramic coating. They included different distribution of segmented primary cracks, secondary crack, large voids and porosity. The lamellas of CYSZ have been formed from interspalts solidification and having porosity as shown from higher magnification SEM photograph (Figure 1). The microstructure of splats is fine cellular structure less than 2 µm (Figure 2). It reflects the rapid solidification mechanism associated with plasma spraying technique. Microstructure analysis of the upper surface plan views of plasma sprayed as clearly revealed from SEM micrographs showed the presence of some unmelted particles and semi melted particles (Figure 3).

Careful analysis of SEM micrographs of upper surface plan views (Figure 4) revealed the wide ranges of sizes of heterogeneous distribution of porosity (open and closed) from approximately higher than 500 nanometers to less than 15 µm. Higher porosity size with lower percentage was observed from the transverse section of CYSZ coat compared with upper surface plan view. The histogram distribution and cumulative% for less than size for open and closed porosity determined from Image J are shown in Figures (5 and 6). The porosities have random shapes due to the solidification of millions of splats. The plasma sprayed coatings also characterized with the presence of random crack networks orientations having different lengths. These differences in microstructure associated with plasma spraying technique have a direct influencing on all physical, chemical and mechanical properties. The volume fractions of open and closed porosity are approximately within 14.9 ± 0.9% and 11 ± 0.3% respectively. The interesting result associated with these scatter in microstructure and defects is the narrow scatter of roughness as confirmed also from Image J (Figure 7). They ranged from approximately 5.2 to 7.2 µm as measured by Talysurf roughness tester. This may reflect the best selection of spraying processing parameters and the difference is technically accepted for the spraying process. Hardness measurements and fracture toughness measurements for many plasma sprayed coatings showed considerable variation of these properties with the same sample or different samples (Figures. 8 and 9). The hardness and fracture toughness of plasma sprayed coating were varied highly within the range of 340 to 870 Hv and 4.8 to 6.5 $MPa.m^{0.5}$ respectively. These are attributed to the heterogeneity of the plasma sprayed coatings associated with low value of Weibull modulus (Tables 2 and 3). The values of Weibull modulus (m) obtained from the plot between lnln ($1/S_i$) and ln hardness (Hv) or ln fracture toughness (K_{IC}) shown in Figs. 8 and 9 are low. These low values of m provide a good measure of high scatter of the hardness and fracture toughness. A direct relation between the values of $\%S_i$ and the property at any value (σ_i) (in this study hardness or fracture toughness) can be described as:

$$S = e\text{-}(\sigma/\sigma_o)^m \qquad (2)$$

where S is equal to 1/e (37%), σ is any value of the given property, σ_o is the value of the given property at value of S equal to 37% (it obtains from the curve) and m is the Weibull modulus (slope of the line from the curve). The above equation described the probability of survival which is very important to select the maximum working property during service should does not exceed corresponding to the given probability of survival.

CONCLUSIONS

1- The different measurements of CLA roughness of upper surface plan views of plasma sprayed coatings showed that roughness can be described effectively using the median value rather than Weibull distribution.
2- SEM analysis of the upper surface plan views of the plasma sprayed coatings revealed the presence of pores with different sizes.
3- The hardness and fracture toughness of the zirconia- 20 wt% ceria- 3.6 wt% yttria changed remarkably due to the presence of porosity, unmelted particles, semimelted particles and crack networks.
4- The values of Weibull modulus of hardness and fracture toughness of plasma sprayed ceramic coatings are low. This modulus is the only parameter to be evaluating to describe the state of the coatings.

Table 1. Processing sheet of shot blasted substrate and plasma sprayed coat of zirconia-ceria-yttria coatings.

Processing sheet of shot blasted		
Substrate	**Ground SiC Inconel IN-738 LC superalloy**	
Blast Pressure	**4 bar**	
Blast distance	**150-200 mm**	
Processing sheet of plasma spraying of thermal barrier coatings		
	Bond coat	**`Ceramic coat**
Primary gas	**Ar**	**Ar**
Pressure, bar	**6.89**	**6.89**
Flow rate, SLPM	**39.95**	**53.25**
Secondary gas	**H_2**	**H_2**
Pressure, bar	**3.44**	**3.44**
Flow rate, SLPM	**6.11**	**7.52**
Current, A , Ampere	**450**	**525**
Voltage (V), Volt	**50**	**55**
Spray distance, mm	**120**	**70**
Angle, %	**90^{o}**	**90^{o}**
Carrier	**Ar**	**Ar**
Flowrate, SLPM	**13.16**	**17.39**
Powder feed rate, g/min	**45**	**35**

Table 2. The distribution of microhardness measurements of as-sprayed coatings and its 37% value obtained from Weibull's distribution.

Reading number	Hv	lnHv	S_i x 10^{-2}	$1/S_i$	$\ln(1/S_i)$	$\ln\ln(1/S_i)$	m	Hv at 37% S_i
1	868	6.76620	4.761905	21.00	3.044522	1.113344	4.241	≈ 596
2	788	6.66950	9.52381	10.5	2.351375	0.855000		
3	684	6.52796	14.28571	7.00	1.94591	0.66573		
4	664	6.49829	19.04762	5.25	1.658228	0.505750		
5	652	6.48005	23.80952	4.20	1.435085	0.361224		
6	640	6.46147	28.57143	3.50	1.252763	0.225351		
7	622	6.43294	33.33333	3.00	1.098612	0.094048		
8	588	6.37672	38.09524	2.63	0.965081	-0.03554		
9	542	6.29527	42.85714	2.33	0.847298	-0.16570		
10	532	6.27664	47.61905	2.10	0.741937	-0.29849		
11	522	6.25766	52.38095	1.91	0.559616	-0.58050		
12	518	6.24997	57.14286	1.75	0.559616	-0.58050		
13	506	6.22653	61.90476	1.62	0.479573	-0.73486		
14	472	6.15697	66.66667	1.50	0.405465	-0.90272		
15	452	6.11368	71.42857	1.40	0.336472	-1.08924		
16	450	6.10924	76.19048	1.31	0.271934	-1.3022		
17	431	6.06611	80.95238	1.23	0.211309	-1.55443		
18	371	5.91620	85.71429	1.17	0.154151	-1.86982		
19	363	5.89440	90.47619	1.11	0.100083	-2.30175		
20	342	5.83481	95.23810	1.05	0.04879	-3.02023		

Table 3. The distribution of fracture toughness measurements of as-sprayed coatings and its 37% value obtained from Weibull's distribution.

Reading number	K_{IC}	ln K_{IC}	S_i x 10^{-2}	$1/S_i$	$\ln(1/S_i)$	$\ln\ln(1/S_i)$	m	K_{IC} at 37% S_i
1	7.22	1.976855	4.761905	21.00	3.044522	1.113344	3.983	5.32
2	6.62	1.890095	9.52381	10.5	2.351375	0.855000		
3	6.48	1.868721	14.28571	7.00	1.94591	0.66573		
4	6.12	1.811562	19.04762	5.25	1.658228	0.505750		
5	5.68	1.736951	23.80952	4.20	1.435085	0.361224		
6	5.83	1.763017	28.57143	3.50	1.252763	0.225351		
7	5.66	1.733424	33.33333	3.00	1.098612	0.094048		
8	5.24	1.656321	38.09524	2.63	0.965081	-0.03554		
9	5.18	1.644805	42.85714	2.33	0.847298	-0.16570		
10	4.64	1.534714	47.61905	2.10	0.741937	-0.29849		
11	4.52	1.508512	52.38095	1.91	0.559616	-0.58050		
12	4.41	1.483875	57.14286	1.75	0.559616	-0.58050		
13	4.36	1.472472	61.90476	1.62	0.479573	-0.73486		
14	4.34	1.467874	66.66667	1.50	0.405465	-0.90272		
15	4.28	1.453953	71.42857	1.40	0.336472	-1.08924		
16	4.21	1.437463	76.19048	1.31	0.271934	-1.3022		
17	3.86	1.350667	80.95238	1.23	0.211309	-1.55443		
18	3.66	1.297463	85.71429	1.17	0.154151	-1.86982		
19	3.18	1.156881	90.47619	1.11	0.100083	-2.30175		
20	2.35	0.854415	95.23810	1.05	0.04879	-3.02023		

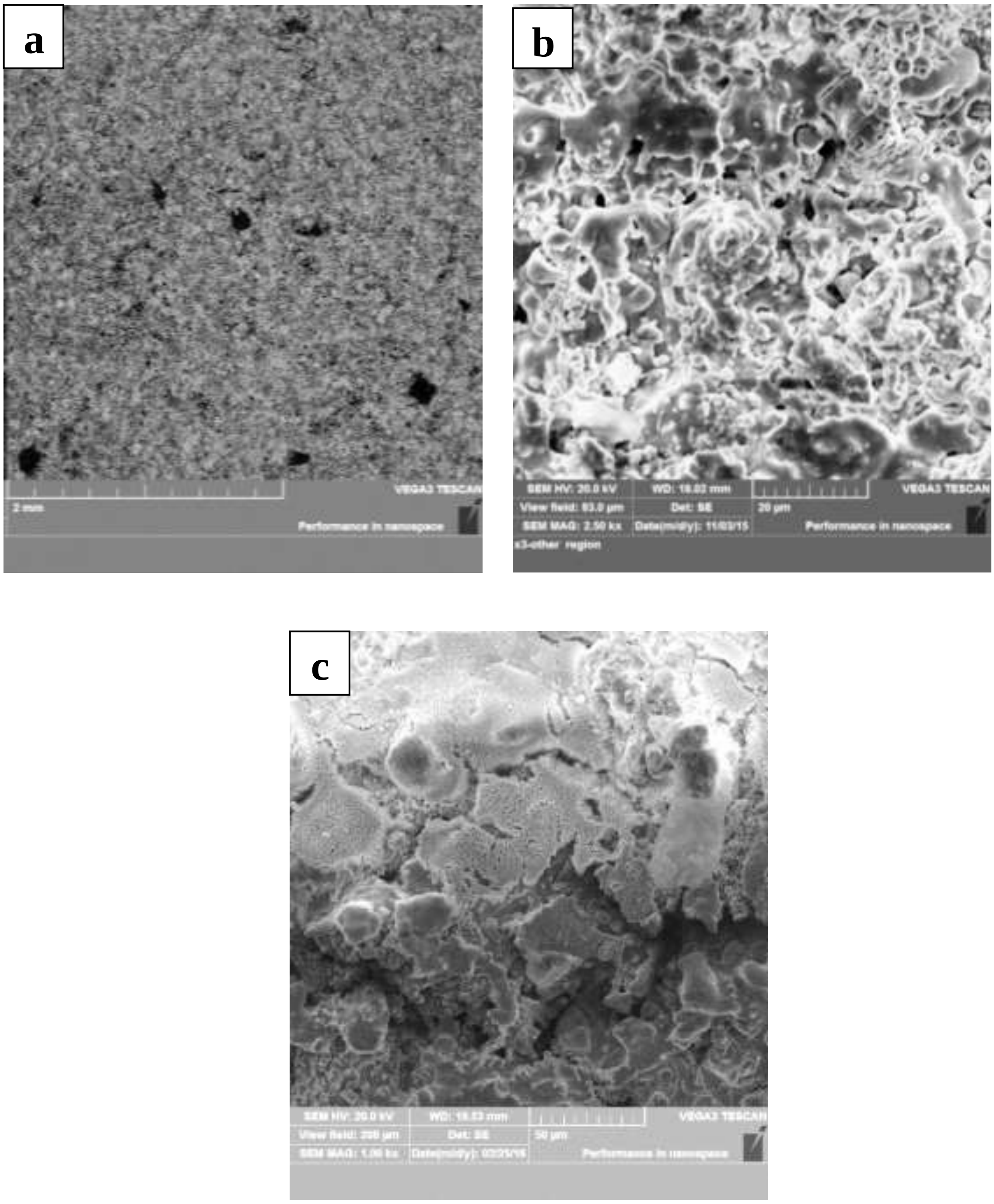

Fig. 1. General upper surface plan view low magnification SEM micrograph of thermal spray zirconia-20 wt% ceria- 3.6 wt% yttria (a), the lamellas of thermal spray CYSZ coatings presenting micro pores and cracks (b) low magnification and (c) high magnification.

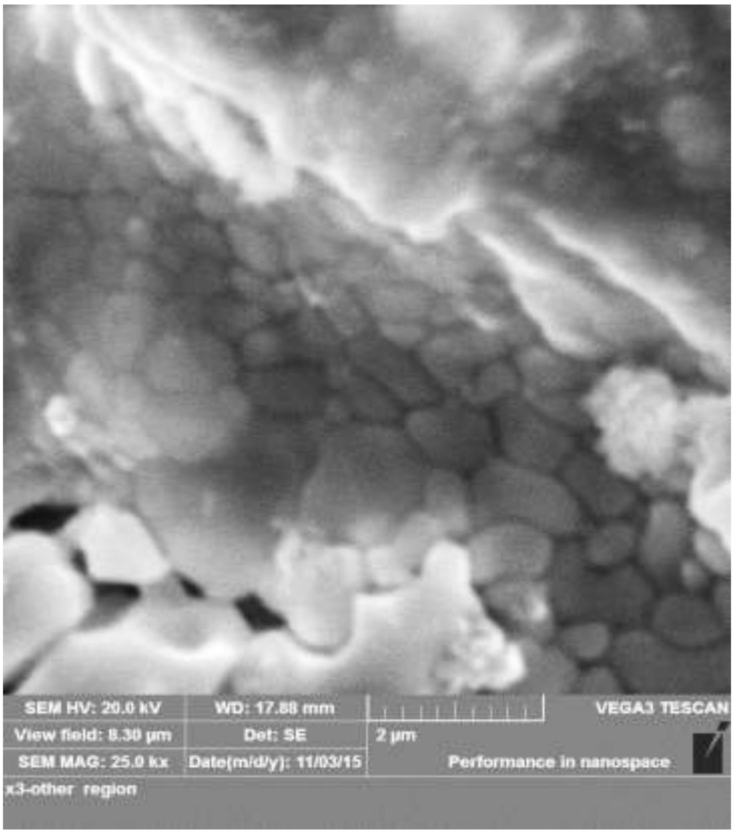

Fig. 2. Typical cellar structure of melted splats observed from upper surface plan view of plasma sprayed CYSZ coating.

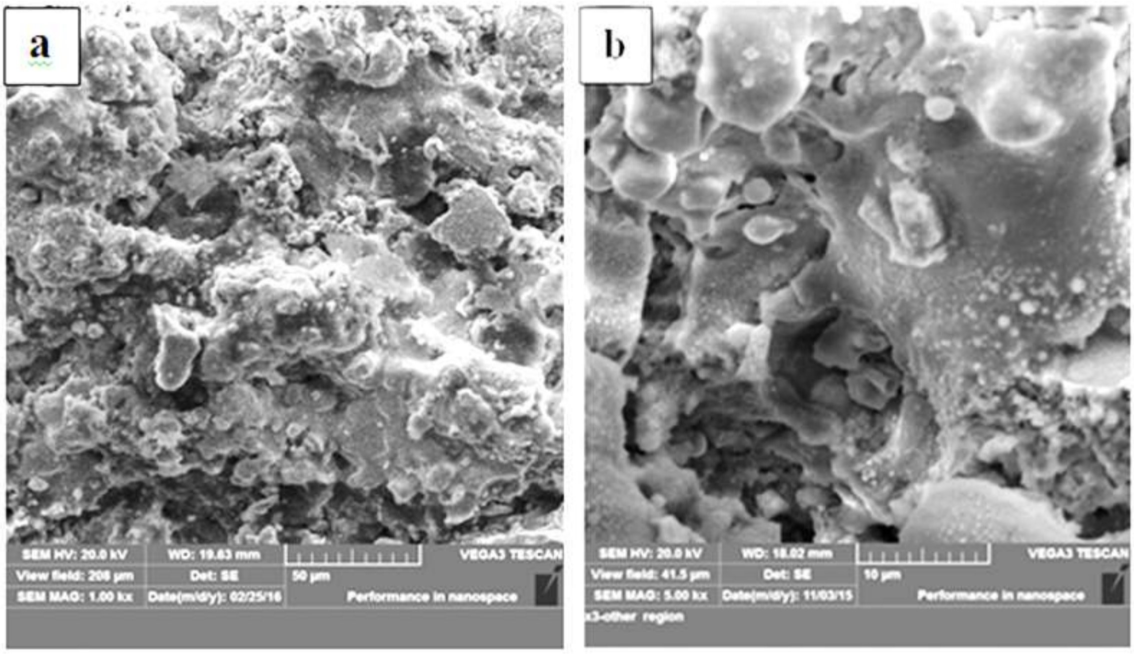

Fig. 3. SEM micrographs of CYSZ plasma sprayed coatings showing the presence of some semimelted and unmelted particles (a) low magnification and (b) higher magnification.

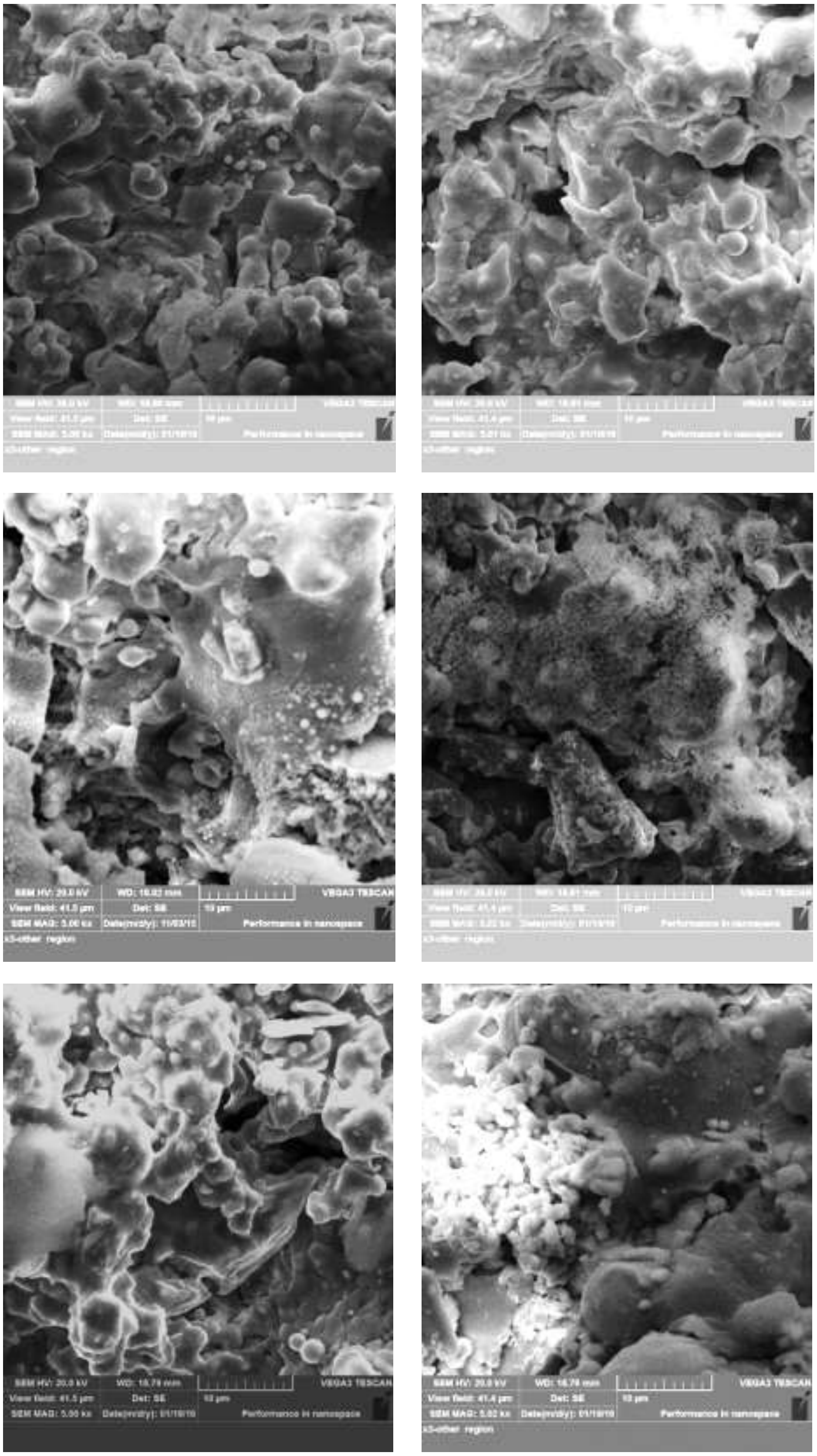

Fig. 4. SEM micrographs of different plasma spray CYSZ coatings showing the scatter of topography and pores.

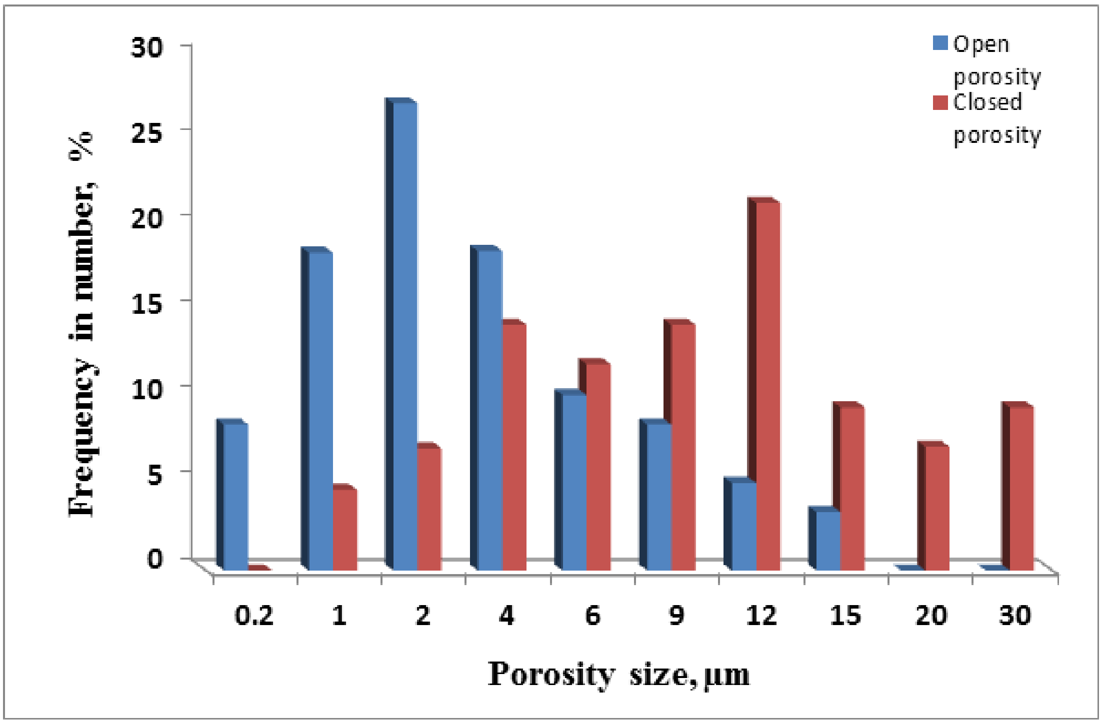

Fig. 5. Histogram distribution open and closed pores.

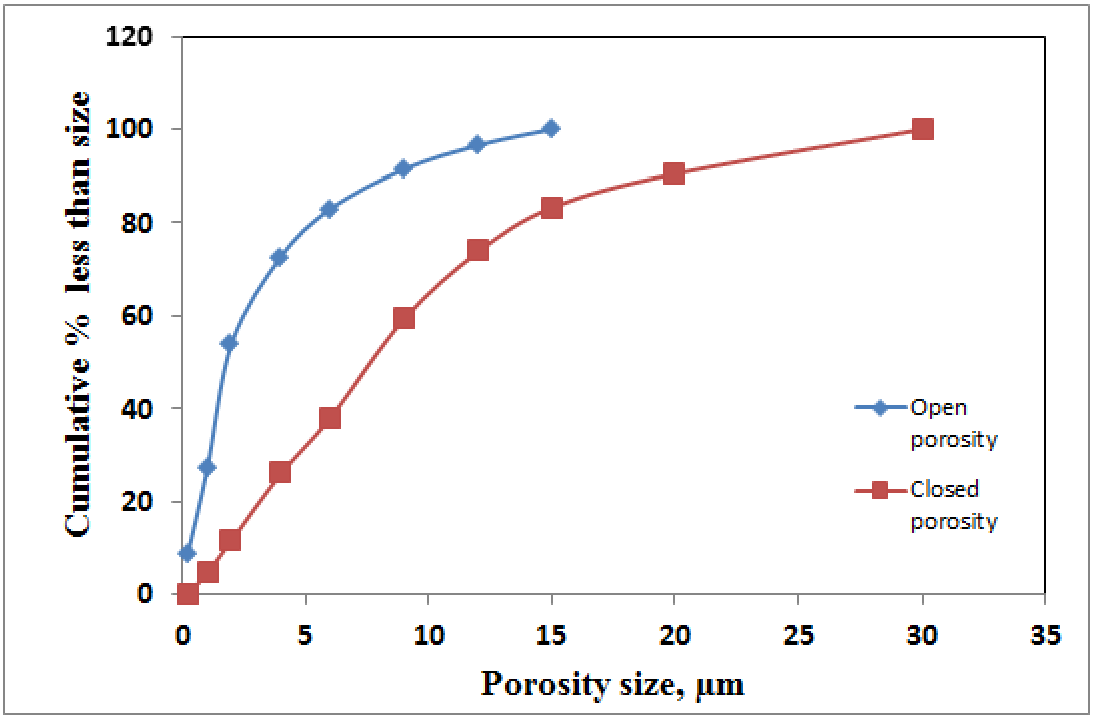

Fig. 6. Cumulative distribution of open and closed pores.

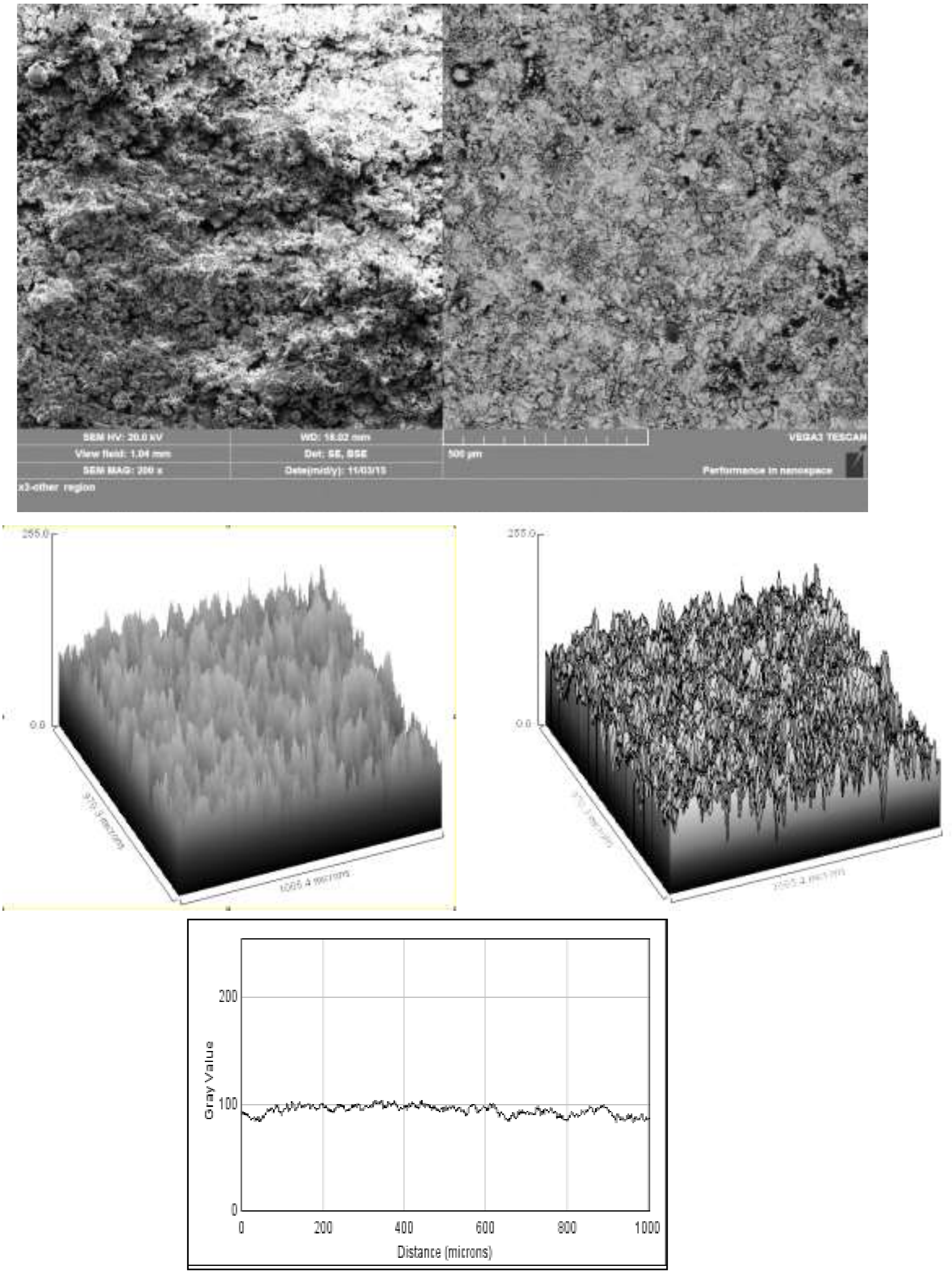

Fig. 7. Appearance of SEM micrographs of as-sprayed upper surface plan view of CYSZ and Image J showing the high roughness.

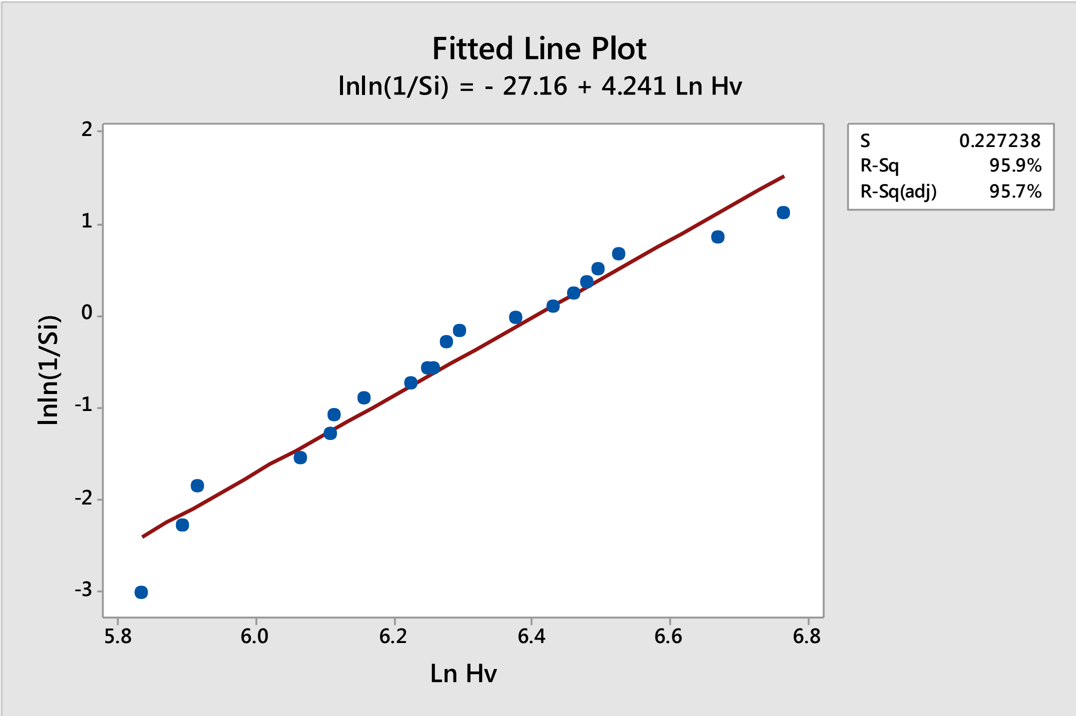

Fig. 8. The Weibull's distribution of hardness of as-sprayed CYSZ.

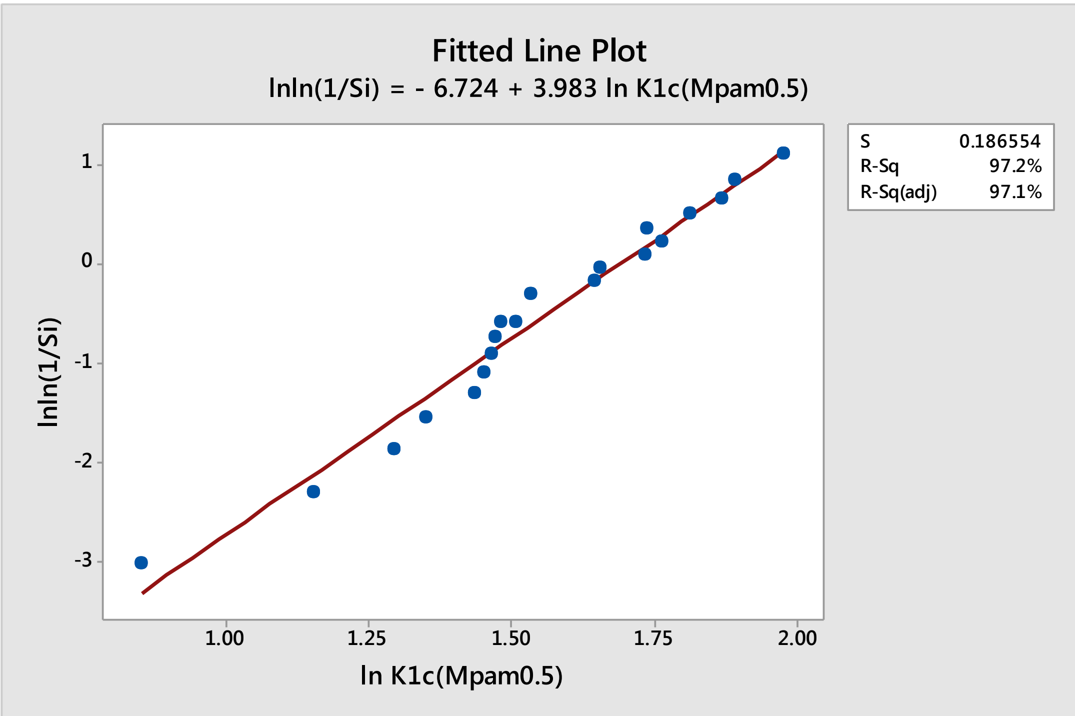

Fig. 9. The Weibull's distribution of fracture toughness of as-sprayed CYSZ.

REFRENCES

Bai Y, Han ZH, Li HQ, Xu C, Xu YL, Wang Z, Ding CH, Yang JF, High performance nanostructured ZrO_2 based thermal barrier coatings deposited by high efficiency supersonic plasma spraying, Applied Surface Science, 257(2011)7210-7216.

Blairbarlett H, Thomas Jr, RR., A study of the mineralogical and physical characterization of two Lithia-zirconia bodies, J of the Ceramic Society, 17(1934)17-20.

Bratton RJ, Lau SK, Zirconia thermal barrier coatings, pp. 226-240 in Advances in Ceramics, Vol. 3, Science and Technology of Zirconia. Edited by A.H. Heuer and L.W. Hobbs. American Ceramic Society, Columbus, OH, 1981.

Chang GC, Phucharoen W, Miller RA, Behavior of thermal barrier coatings for advanced gas turbine blades, Surface and Coatings Technology, 130(1987)13-28.

Christian Coddet. ASM International, Materials Park, OH, USA, 1998, pp. 1669-1673.

Duwez P, Brown JR FH, Stabilizing of zirconia with calcia and magnesia, J. of the American Ceramic Society, 35(1952)107-113.

Girolamo GD, Blasi C, Schioppa M, Tapfer L, Structure and thermal properties of heat treated plasma sprayed ceria- Yttria co-stabilized zirconia coatings, Ceramics International, 36(2010)961-968.

Golosnoy IO, Cipitria A, Clyne TW, Heat transfer through plasma-sprayed thermal barrier coatings in gas turbines: A review of recent work, J. Thermal Spray Technology, 18(2009)809-821.

Hajizadeh Oghaz M, Shoja Razavi R, Ghasemi A, Valefi Z, Na_2SO_4 and V_2O_5 molten salts corrosion resistance of plasma sprayed nanostructured ceria and yttria co-stabilized, Ceramics International, 42(2016)5433-5446.

Lee CH, Kim HK, Choi HS, Ahn HS, Phase Transformation and bond coat oxidation behavior of plasma sprayed zirconia thermal barrier coatings, Surface and Coating Technology, 124(2000)1-12.

Miller AR, Thermal barrier coatings for aircraft engines: history and directions. J. of Thermal Spray Technology, 6(1997)35-42.

Ponton CB, Rawlings RD, Vickers indentation fracture toughness test Part 1 Review of literature and formulation of standardized indentation toughness equations, Materials science and Technology, 5(1989)865-871.

Ramachandran CS, Balasubramanian V, Ananthapadmanabhan PV, Viswabaskaran V, Influence of the intermixed interfacial layers on the thermal cycling behavior of atmospheric plasma sprayed lanthanum zirconate based coatings, Ceramics International, 38(2012)4081-4096.

Saremi M, Afrasiabi A, Kobayashi A, Microstructural analysis of YSZ and YSZ/Al_2O_3 plasma sprayed thermal barrier coatings after high temperature oxidation, Surface and Coatings Technology, 202(2008)3233-3238.

Strangman TE, Schienle JL, Tailoring zirconia coatings for performance in a marine gas turbine environment, J. of Engineering Power (Trans. ASME), 112(1990)531-535.

Tsipas SA, Effect of dopants on the phase stability of zirconia-based plasma sprayed thermal barrier coatings, J. of the European Ceramic Society, 30(2010)61-72.

Wang Y, Sayre G, Commercial thermal barrier coatings with a double-layer bond coat on turbine vanes and the process repeatability, Surface and Coatings Technology, 203(2009)2186–2192.

Wang L, Wang Y, Sun XG, He JQ, Pan ZY, Zhou Y, Wu PL, Influence of pores on the thermal insulation behavior of thermal barrier coatings prepared by atmospheric plasma spray, Materials and Design, 32(2011)36-47.

Wang L, Wang Y, Sun XQ, He JQ, Pan ZY, C.H. Wang CH, Thermal shock behavior of 8YSZ and double-ceramic-layer $La_2Zr_2O_7$/8YSZ thermal barrier coatings fabricated by atmospheric plasma spraying, Ceramics International 38(2012)3595-3606.

Wilden J, Wank M, Steffens HD, Brune M, New thermal barrier coating system for high temperature applications. In Proceedings of the 15th International Thermal Spray Conference: Thermal Spray Meeting the Challenges of the 21st Century, Nice, France, May 1998.

Zhou F, Wang Y, Cui Z, Wang L, Gou J, Zhang Q, Wang C, Thermal cycling behavior of nanostructured 8YSZ , SZ/8YSZ and 8CSZ/8YSZ thermal barrier coatings fabricated by atmospheric plasma spraying, Ceramics International, 43(2017)4102-4111.